Energy and Earth Science
Vol. 6, No. 2, 2023
www.scholink.org/ojs/index.php/ees
ISSN 2578-1359 (Print) ISSN 2578-1367 (Online)

Original Paper

Detection of Ring Structures and Their Surrounding Tectonic Pattern in South-Algeria, North-Mali and North- Niger based on Satellite Data

Barbara Theilen-Willige[1]

[1] Technische Universität Berlin (TUB), Faculty IV (retired), Berlin, Germany

Received: March 21, 2023 Accepted: March 30, 2023 Online Published: April 25, 2023
doi:10.22158/ees.v6n2p1 URL: http://dx.doi.org/10.22158/ees.v6n2p1

Abstract

This study is focused on the detection of circular features with different sizes, origins, and state of erosion as well as on their surrounding tectonic pattern based on different satellite images of Southern Algeria, Northern Mali and Northern Niger. Sentinel 2- and Landsat 8/9-images and Sentinel 1- and ALOS L-band Phased Array Synthetic Aperture Radar (PALSAR)-radar data help to identify larger ring structures and smaller circular features, most of them related to magmatic intrusions into the subsurface, but also to cosmic impacts, with varying ages and state of erosion. Some of them seem to be unknown so far as they are partly covered by aeolian sediments and become only visible on radar images. Digital Elevation Model (DEM) data and the DEM derived morphometric maps support these investigations in a GeoInformation System (GIS) embedded environment. Some of the ring structures are only visible on morphometric maps, traced by circular arrangements of slope gradients or concentric drainage patterns. The large, circular structures and the smaller circular features such as volcanic features (cinder cones, calderas, maars, impact craters) were digitized and merged in a GIS with available geologic information.

Keywords

ring structures, structural analysis, remote sensing, S-Algeria

1. Introduction

Although a large amount of research has been carried out related to the geologic history and structural and tectonic inventory in Southern Algeria and adjacent areas (Liégeois et al., 2005; Azzouni-Sekkal et al., 2007; Fezaa et al., 2010; Yahiaoui et al., 2014; Bouzid et al., 2015) combined evaluations of different satellite data integrated into a GeoInformation System (GIS) are investigated, whether they can contribute to further additional geologic knowledge Especially the combination of Landsat 8 and 9 thermal band-, and Sentinel 2 optical images, and Sentinel 1-, ALOS PALSAR- and SIR-C-radar images allows the detection of surface-near structures (Paillou et al., 2006).

After evaluations of optical and radar satellite images and digital elevation data from Southern Algeria, Northern Mali and Northern Niger it became obvious, that there are some circular structures visible on the satellite images and on morphometric maps that were neither documented on available geologic maps, nor described in the geologic literature and, thus, seem to be unknown so far. The reasons for this vary according to the specific situation. Some structures are buried underneath younger sediments and extended aeolian covers and not visible in the field, but still on satellite radar data because of the concentric arrangement of the drainage pattern or ring-shaped tonal anomalies on the images. Therefore, this study aims to contribute to the systematic detection and inventory of ring structures and their adjacent tectonic pattern, as far as possible based on remote sensing and GeoInformation System (GIS) methods.

The combination of different remote sensing data is used in the scope of this study to derive an overview of structural information and focus on an inventory of circular features of different sizes and origins and their surrounding tectonic pattern. Such an inventory is important for example for hydrogeologic investigations as the groundwater flow is influenced by those structures because of permeability changes and for the mining and energy industry. For example, larger ring structures have an impact on multi-aquifer groundwater flow in the different groundwater levels. The larger fault systems and geologic structures such as dikes affecting the groundwater flow should be mapped carefully using the potential of thermal and radar satellite data as far as possible for this purpose. The long and thick, low-permeability dikes often act as barriers for the topography-driven groundwater flow.

As mineral occurrence and deposits of economic value are often related to ring structures evaluations of satellite data might be of use for further detailed exploration.

Another reason for the detailed inventory of circular structures is the monitoring of potential geohazards. The position of larger ring structures related to plutons seem to have an influence on earthquake activity (Theilen-Willige, 2022). The different circular forms created by volcanic activity might be a risk for the land use and infrastructure, even in this arid environment with a low population density. Not only the smaller eruptions have to be considered, but also the numerous dikes along fault zones and zones of weakness along structures.

Another example for the importance of geohazard monitoring is the collapse of sinkholes in karst areas affecting the safety of infrastructure.

Among the geohazards cosmic impacts of a larger meteorites or even asteroids have to be taken into account as well. The documented impact craters in Algeria, Mali and Niger are proof of this potential risk in the geologic history. The Earth Impact Database (EID) created by the Planetary and Space Science Centre (PASSC), Canada, comprises a list of confirmed impact structures from around the world on land surfaces. To date, there are 190 confirmed impact structures in the world-wide database. It can be assumed that with ongoing research further impact craters will be discovered, some of them may be in the scope of this study. The low settlement density and land use restricted to water availability in this arid environment allows the conservation of craters, although often covered by aeolian sediments. Special attention is focused on smaller, bowl-shaped craters that can be related to volcanic maars and calderas, karst depressions or impact craters.

The next figure shows an overview of cosmic impact craters in the investigation area covering Algeria and N-Mali and N-Niger (Figure 1).

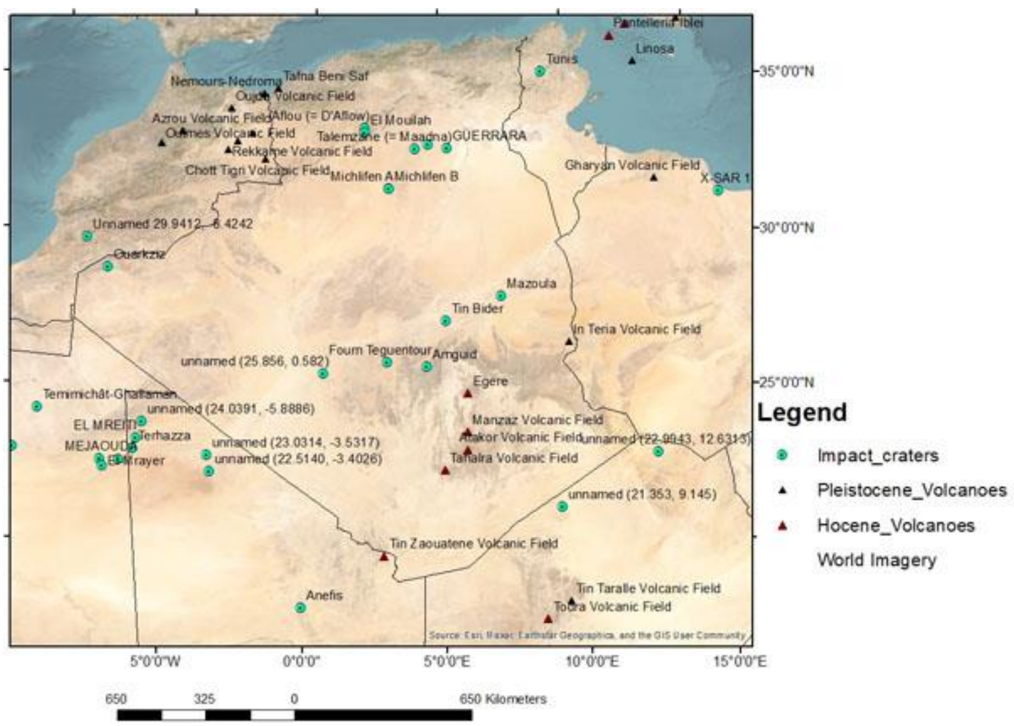

Figure 1. Overview of Documented Impact Craters in Algeria. N-Mali and N-Niger Based on the Planetary and Space Science Centre (PASSC), Canada, Impact Crater Data Base

2. Geographic and Geologic Overview

The investigation area includes the Hoggar mountains in S-Algeria with height levels up to 2900 m, the Air mountains in N-Niger reaching height levels up to 2000 m and the Adrar des Iforas in NE-Mali with height levels between 800-900 m (Figure 2). The climate is characterized by an arid environment with a hot desert climate.

The Hoggar Massif in Algeria is associated with exposed Pan-African basement extending over an area greater than 500 000 km^2 (English et al., 2016), belonging to the Tuareg Shield composed of terranes. Most of the Tuared Shield is situated in Algeria (Hoggar) and extends in the SW into the Adrar des Iforas in Mali mountains and in the SE into the Air mountains in Niger. The Hoggar mountains form the main part of the Tuareg shield, which principally comprises Archaean/Palaeoproterozoic and Neoproterozoic terranes, composed of Precambrian lithologies and unconformably overlain by subhorizontal Palaeozoic sediments. The Tuareg shield amalgamated during the late Neoproterozoic Pan-African orogeny as a result of the convergence of the West African craton (WAC) and the Saharan craton. The major structural domains of the Tuareg Shield are the “Polycyclic Central Hoggar” to the east and the “Western Hoggar”, or “Pharusian Belt”, to the west (Kourim et al., 2014). The terranes collided, welded and moved along subvertical shear zones to be finally squeezed between the West African craton to the west and the Saharan metacraton to the east (Azzouni-Sekkal et al., 2003).

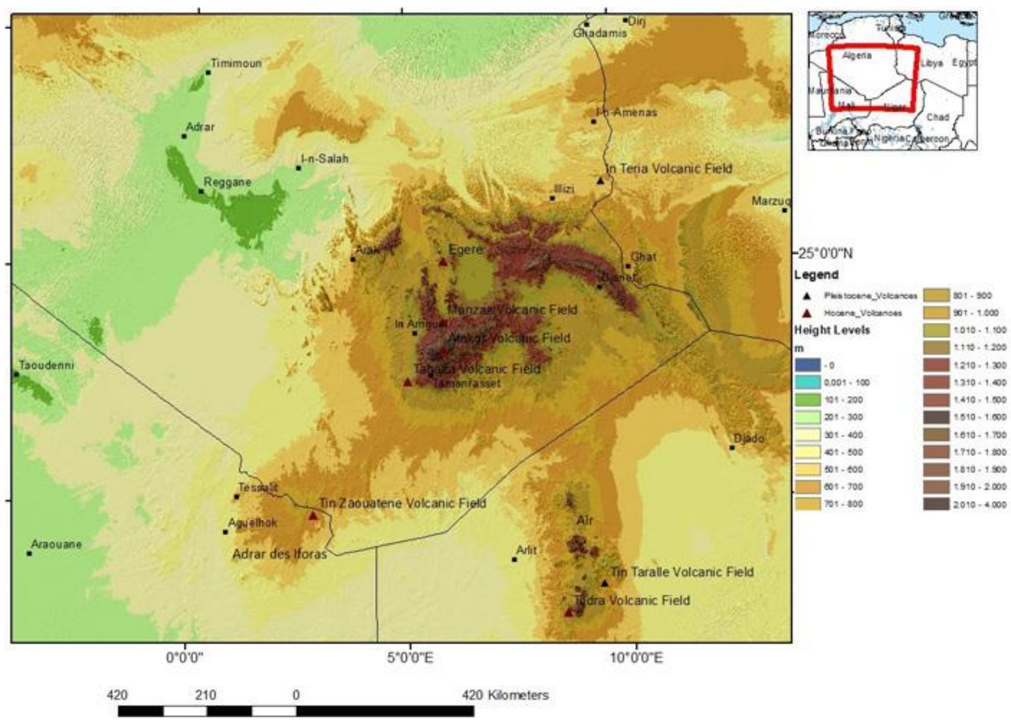

Figure 2. Height Level Map of the Investigation Area Based On GEBCO Elevation Data

Geochronological results demonstrate that the Eastern Hoggar had not stabilized by c. 730 Ma, but was subjected to a late Ediacaran tectono-magmatic episode at c. 575-555 Ma. This episode is younger and unlinked to the Pan-African orogeny that occurred further west in the Tuareg Shield (Fezaa et al., 2010). A first stage comprised the accretion of oceanic island arcs on these cratons and on microcratons during the period 900-680 Ma. Relics of these terranes, including ophiolites and eclogites, are preserved as thrust sheets on more rigid bodies (Liégeois et al., 2003, 2008). The second stage was the regional northerly tectonic escape of the Tuareg terranes due to oblique collision with the WAC. During that stage, the metacratonization of the Central Hoggar microcontinent occurred, the squeezing of this rigid body, which was torn into several moving blocks. During the main Pan-African phase (625-580 Ma) the Central Hoggar microcontinent was dissected by N-S-oriented mega-shear zones that induced several hundreds of kilometers of relative displacement and allowed the emplacement of high-K calc-alkaline batholiths. Smaller movements continued till 525 Ma, accompanied by the emplacement of subcircular plutons with alkaline affinity. Linear lithospheric delamination beneath these mega-shear zones may occur under such circumstances, allowing a drastic increase in heat flow and melting of the crust. Post collisional and anorogenic high-level alkaline plutons are aligned on the same megashear zones, particularly along craton margins (Liégeois et al., 2003; Fezaa et al., 2010).

Figure 3 provides a geologic overview of the main geologic units according to the data provided in the web portal OneGeology by the British Geological Survey British Geological Survey (BGS).

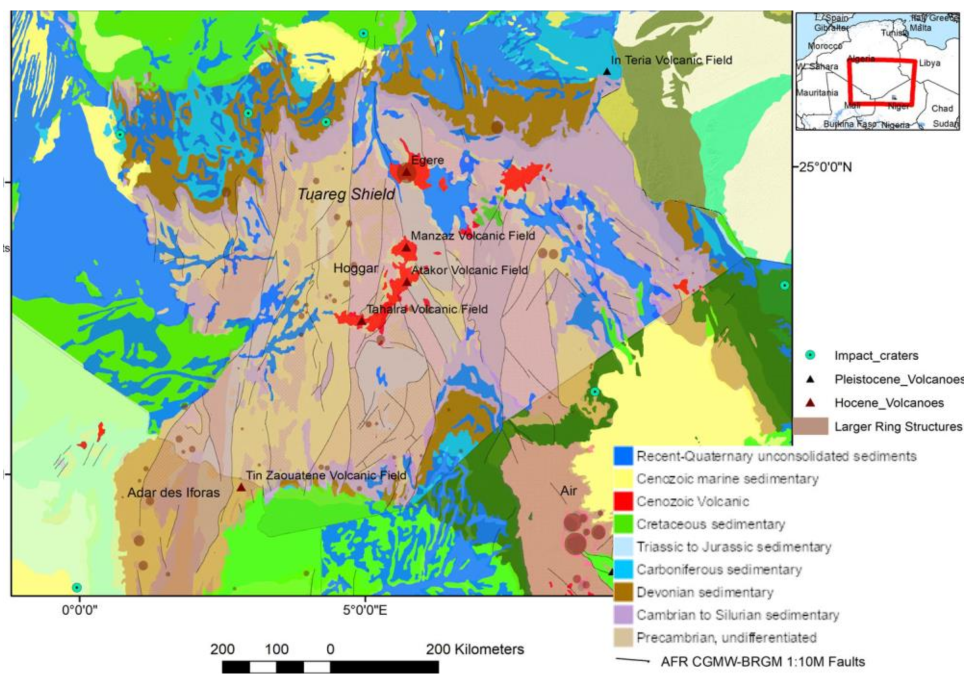

Figure 3. Geologic Overview of the Tuareg Shield according to the 1:10M-scale Geological Map of Africa-BGS, 1:5,000,000 Scale, Downloaded from the OneGeology, http://portal.onegeology.org/OnegeologyGlobal/

Recent volcanic activity from Upper Eocene to Quaternary in age (35 to nearly 0 Ma) is associated in the Hoggar area with a crustal swell of 1000 km in diameter, probably the product of a mantle plume. In response to stress resulting from the Africa-Europe collision, volcanism may be generated by adiabatic pressure release of an uprising asthenosphere. The reactivation of preexisting shear zones and fractures generated during the Pan-African (late Neoproterozoic) orogeny (inducing limited linear lithospheric delamination at the lithosphere-asthenosphere interface along these mega-shear) played an important role. There are several volcanic districts located in Hoggar, Massif, N-Mali and N-Niger (Figure 3, Liégeois et al., 2003, 2008; Yahiaoui et al., 2014; Bouzid et al., 2015). The first volcanic event produced Miocene composite flood lavas (plateau basalt) essentially made of alkali olivine basalts. Trachytic and phonolitic plugs are associated with this phase zones (Liégeois et al., 2003, 2005).

3. Data and Methods

The interdisciplinary approach used in the scope of this research comprises evaluations of remote sensing data, geological, and topographic data, integrated into a GIS environment. Satellite imageries and Digital Elevation Model (DEM) data were used then for generating a GIS data base and combined with different geodata (infrastructure, land use) and available geologic maps. Infrastructural and land use shapefiles from Algeria were downloaded from the Geofabrik's download server.

Digital Elevation Model (DEM) data from the Shuttle Radar Topography Mission (SRTM), and ASTER DEM data (both with about 30 m spatial resolution) are covering the whole investigation area. The Advanced Land Observing Satellite-1 (ALOS), Phased Array type L-band Synthetic Aperture Radar (PALSAR) from the Japan Aerospace Exploration Agency (JAXA) provided data with 12.5 m spatial resolution, however, not a complete coverage. The satellite data were downloaded from open sources such as the USGS/Earth Explorer, the Sentinel Hub/ESA, and the Alaska Satellite Facility (ASF).

3.1 Digital Image Processing of Different Optical and Radar Satellite Data

Satellite data were processed and evaluated such as Sentinel 1-C-Band, Synthetic Aperture Radar (SAR) and ALOS PALSAR L-Band data and optical Sentinel 2 images, and Landsat optical data (Landsat TM and Landsat 8 and 9 of the Operational Land Imager-OLI) using digital image processing software as the Sentinel Application Platform (SNAP)/ESA and ENVI/L3Harris Geospatial Solutions as well as the geoinformation systems ArcGIS/ESRI and QGIS. Digital image processing of LANDSAT 5 Thematic Mapper and Landsat 8/9-The Operational Land Imager (OLI) data was carried out by merging different Red Green Blue (RGB) band combinations with the panchromatic Band 8 to pan-sharpen the images. Three color composites were generated for the purpose of lithological zones mapping. Especially, when combing the thermal bands of optical satellite data in a RGB image structural features are enhanced due to brightness differences. When analyzing satellite data traces of structures such as faults, folding and domes are often clearly visible on satellite images.

By using the band combination of 2, 7 and 10 of Landsat 8/9 even deeply eroded ring structures can become visible as demonstrated by the example below from N-Mali (Figure 4). SNAP from ESA provided the tools as well for the processing of radar data.

Synthetic Aperture Radar (SAR) space-borne satellites operate by using microwave radiation with a frequency in a range of wavelengths, for example, the L-band (23 cm-1.30 GHz and 24 cm-1.25 GHz), C-band (6 cm-5.0 GHz), (Mansour et al., 2022). L-band radar coverage was acquired by the JERS-1 satellite of the Japanese space agency (JAXA), C-Band coverage by the Sentinel 1 mission of ESA. SAR imagery can differentiate topographic variation with a high spatial resolution. Radar imagers send out pulses of radio waves and collect the return signals after the waves were reflected of surfaces. The smoothness, roughness, and density of a surface affect the return signal. Unlike optical instruments, which can only see the surface, radar can penetrate loose, dry materials such as sand sheets. ALOS/PALSAR L-Band data are characterized by the optimal conditions of penetration in desert areas depending on the grain size, moisture, roughness of the surrounding geology and radar backscattering mechanism (Mansour et al., 2022). In very dry soils, L-Band SAR (1.25 GHz) can intrude into the subsurface down to several meters. Dark image tones are associated in general with flat areas because the incident radar signals were largely reflected from their “radar-smooth” surfaces in a mirror-like fashion away from the satellite antenna.

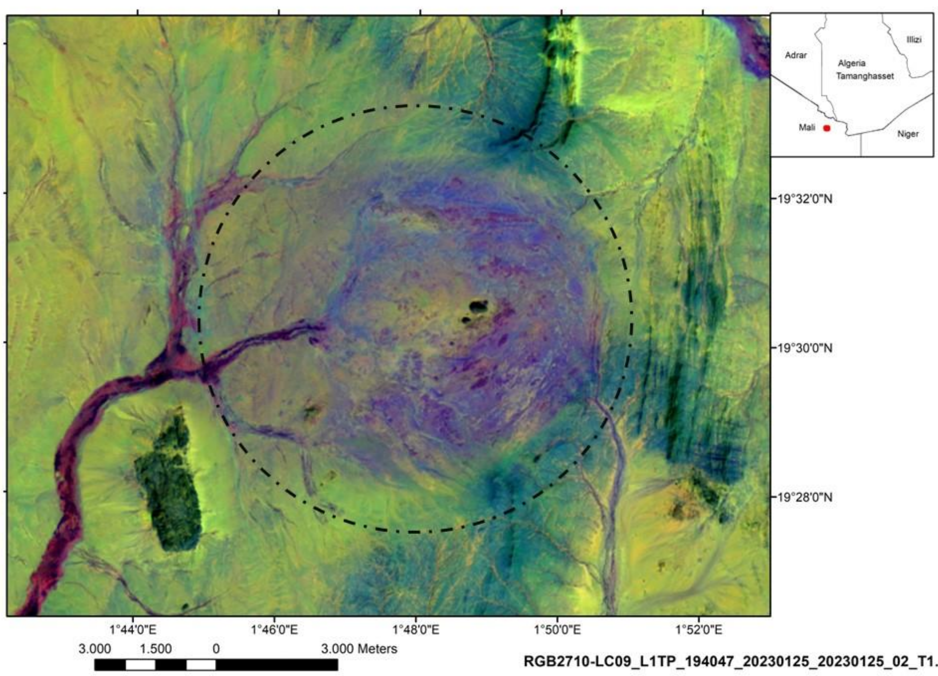

Figure 4. Deeply Eroded Ring Structure in N-Mali Visible on a Landsat 9-Scene (RGB, Bands 2,7 and 10)

Paleodrainage systems become visible due to their radar-smooth reacting sediment fill. Thus, ring structures forming circular basins and depressions are often clearly detectable on radar images. The evaluation of radar data also helps in the building of more complete geological maps and in support of future water and mineral prospecting in arid regions (Paillou et al., 2006, 2017). Evaluations of C- and L-Band radar data prove to be of great value in the arid environment of the investigation area for the detection of geologic structures underneath aeolian covers. The visibility of ring structures on radar images depends in this arid environment mostly on the radar-illumination geometry and the surface properties.

3.2 Evaluations of DEM Data

Mosaics were created based on the various DEM data. In the scope of this study evaluations of morphometric maps derived from different DEM data play an important role because ring structures sometimes can be traced more clearly on slope gradient, height level or drop raster maps than on other satellite images. Optical, digital processed and enhanced satellite images are then correlated with the morphometric maps. Figure 5 shows an example of a combined analysis of different satellite data.

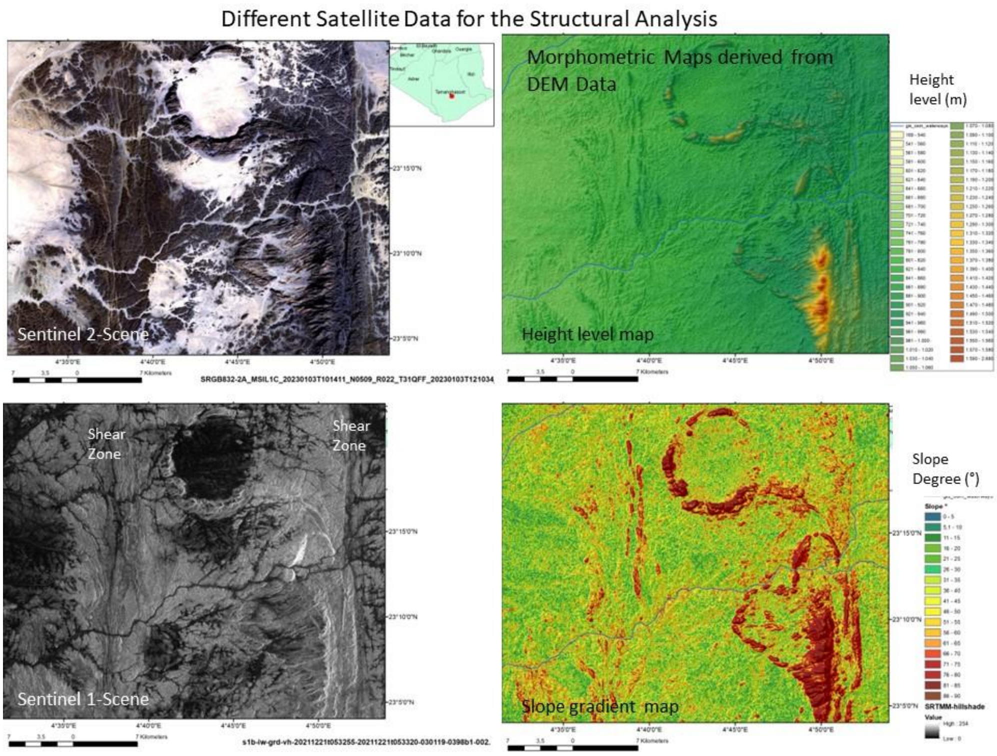

Figure 5. Combined and Comparative Analysis of Different Satellite Data (Optical Data-Sentinel 2, Radar Data-Sentinel 1, SRTM DEM Derived Height Level and Slope Map) for the Detection of Ring Structures and-S-striking Shear Zones

3.3 Structural Evaluation

The shapefiles related to ring structures, lineaments, structural features, karst phenomena and volcanic features were digitized visually based on the different satellite images. Especially Sentinel 1 and ALOS PALSAR radar images reveal larger fault zones, for example by dislocations of lithologic units that can be digitized easily. In the scope of this study the following types of linear and curvilinear features were mapped: lineaments (as a neutral term for linear features without identifying their origin), probable fault zones, major fault zones and structural features. As traces of structural features are digitized the deformations due to stress such as synclines or anticlines, bedding structures, or traces of foliation in metamorphic rocks, often become visible as dense, arc-shaped, parallel lines.

4. Inventory of Ring Structures and Their Surrounding Structural Pattern Based on Satellite Data

In the following chapters an overview of different circular structures and their expressions on satellite images is presented. In most cases their origin can be derived, however, in some cases clarifying of their origin remains for future investigations. The multiple overprinting of the structures during their geologic history often has led to a complex lithologic and tectonic development and composition. The structural pattern was analyzed, whereby the numerous dikes and dike swarms in the investigation area are of great value as the dikes indicate zones of “weakness” allowing the intrusion of magma. The spatial arrangement of mostly basic and ultrabasic dikes, their orientation and their density provide hints about the dynamic stress pattern. When digitizing the circular, structural features, it can be subdivided between several types of ring structures:

a) traces of larger ring structures by a circular outline of the drainage pattern and circular tonal anomalies on the satellite images such as shown in Figure 6,

b) distinct expressed larger ring structures related to plutonic rocks forming often high-altitude domes and hills in the landscape with circular outline (Sieber & Theilen-Willige, 1984),

c) large circular basins with surrounding concentric hill ranges. Some are forming bowl-shaped craters. The origin of this type of ring structure can be complex. One explanation might be volcanic activity leading to the development of a caldera. Another one might be the erosion of a pluton with different resistivity of the lithologic units to erosion. Along concentric faults of plutons magma often intruded later building ring dikes.

d) Smaller volcanic features such as volcanic cones, bowl-shaped craters (often related to maars and some to cosmic impact craters) and undefined smaller depressions such as deflation hollows.

The main types of ring structures according to their sizes, geomorphologic appearance and origin are summarized in Figure 6.

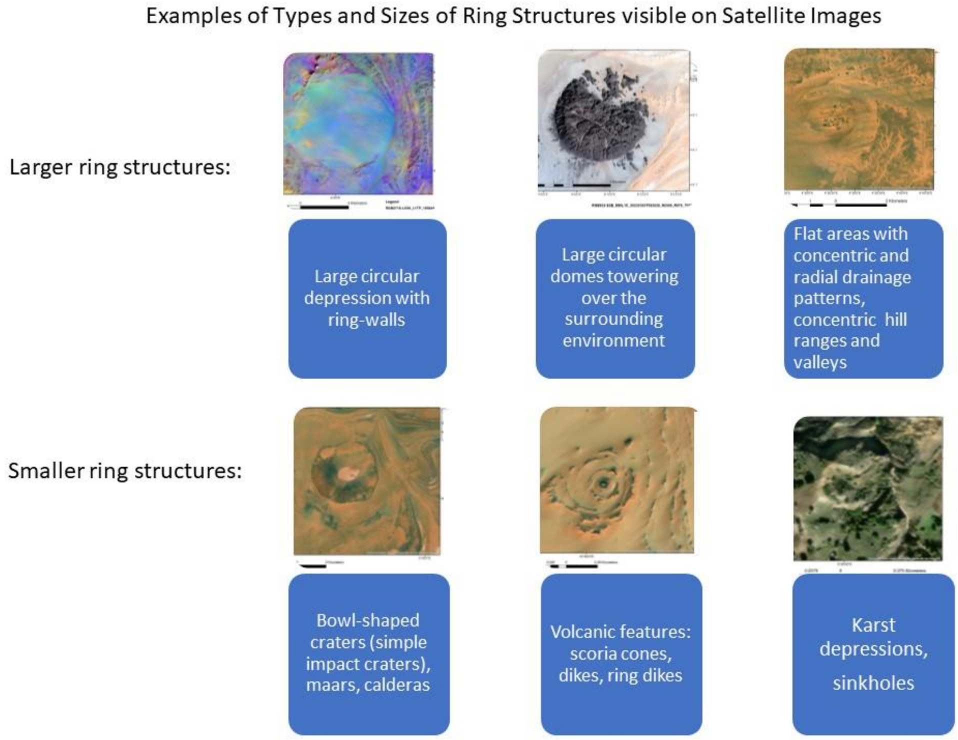

Figure 6. Main Types of Sizes and Origins of Ring Structures

Figure 7 provides an overview of the mapped circular features. Of course, due to the large dune fields and aeolian covers this inventory based on satellite images cannot be complete. When combining the inventory of ring structures with lineament analysis and the known fault systems extracted from geologic maps, it becomes obvious that the larger ring structures are concentrated along the major shear zones (Figure 7). Post collisional and anorogenic high-level alkaline plutons are aligned on these mega-shear zones (Black et al., 1979; Liégeois et al., 2003, 2005, 2007). The NNW-SSE, NNE-SSW and N-S-oriented Pan-African mega-shear zones are cross cutting lithologic units over hundreds of kilometers, up to 1000 km from Middle Algeria to Northern Niger and Mali, visible even through the youngest sedimentary covers. These shear zones consist of parallel segments, partly moving relatively to each other. Sometimes “graben-like” structures can be observed on the satellite images and on height level maps. Recent tectonic uplift might be the reason (Azzouni-Sekkal et al., 2007). The large shear-zones were reactivated during later orogenic events and are still overworked by ongoing neotectonic movements, traced by abrupt displacements and magmatic intrusions, especially by parallel, linear dikes. The shear zones have been displaced and intruded by magmatic bodies forming dikes, maars and scoria cones, most of them of Pleistocene and Holocene ages (Liégeois et al., 2005; Yahiaoui et al., 2014). Dikes and single, smaller volcanic scoria cones occur concentrated along the shear zones, as well as along larger ring structures.

As these shear zones played an important role for the emplacement of magmatic bodies, a more detailed analysis of their structure was carried out using Landsat 8 and 9, Sentinel 2 and radar satellite data. Figure 8 demonstrates the appearance of a shear zone near the southern border of Algeria as visible on a Landsat 9 RGB scene and Figure 9 its structural evaluation.

The varying geomorphologic properties of the shear zones depend on the regional geomechanical stress situation and lithologic composition. Dikes intruded later into shear zones are forming linear ridges over long distances. Reactivations of pre-existing fault structures under the current tectonic stress field have an impact on the development of dikes.

The topographic cross section of the shear zone shown in Figure 9 and reveals the almost flat environment, intersected by ridges and hill chains whenever dikes intruded into these zones of weakness (Figure 10). However, most of them are buried underneath sedimentary covers. Whenever the loose sedimentary covers or other lithologic layers comprise more than several meters, they cannot be detected even on L-Band radar images. The fact that distinct expressed N-S-striking fault zones are clearly visible on the different satellite images, cross-cutting youngest sediments, as well as the intrusion of numerous dikes and scoria cones into the fault segments seems to support the assumption that the shear zones are still reactivated due to ongoing tectonic stress and movements.

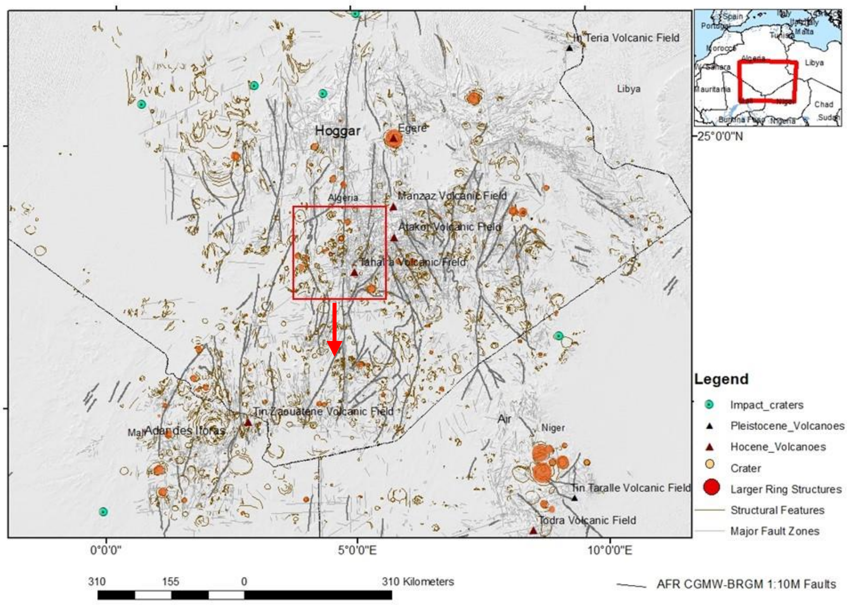

a)

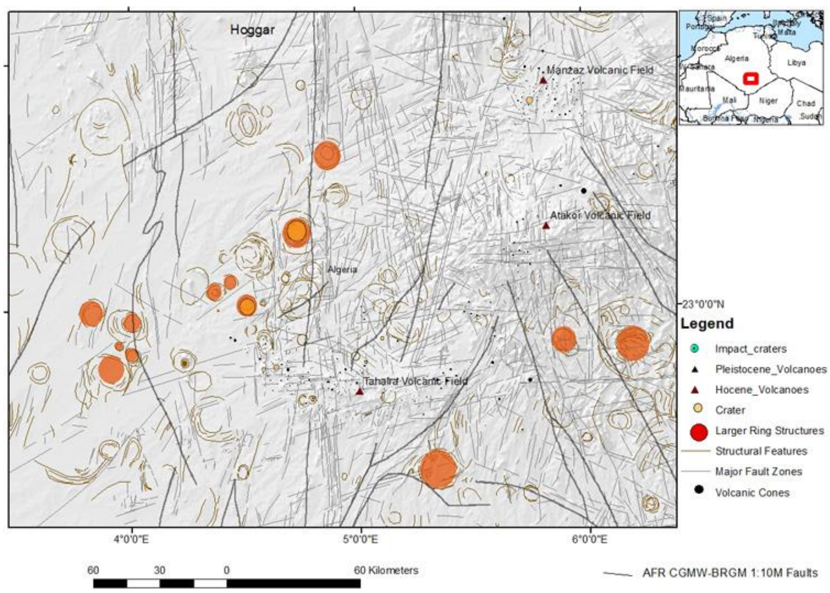

b)

Figure 7 a and b. Structural Evaluation Combined with Known Fault Zones Pan-African Mega Shear Zones, 1:10M-Scale Geological Map of Africa-SIGAfrique-Bedrock Age, French Geological Survey (BRGM), France), Downloaded from the OneGeology Portal

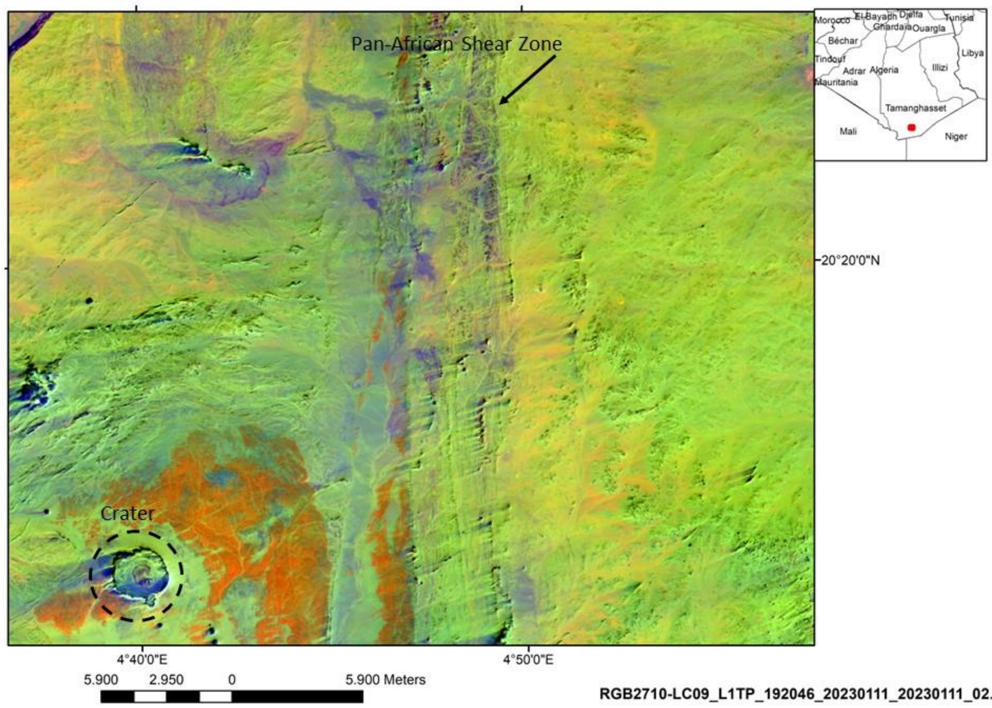

Figure 8. Landsat RGB, Bands 2,7 and 10 Scene of the Shear Zone and a Distinct Visible Crater on the Lower Left of the Scene. The WSW-ENE Oriented Stripes Are Caused by Wind Erosion

The topographic W-E-profile of the crater and the shear zone is presented in Figure 10. The crater rises above the environment with more than 100 m. The height levels of the shear zone vary with the dike occurrence.

Another part of the Pan-African shear zone in the central part of the Hoggar Massif between 4° and 5° longitude is revealed by ALOS PALSAR L-Band data (Figure 11 a-d). The parallel segments can be detected clearly. Dikes are visible as very light lines along the shear zone due to their strong radar backscatter.

In the volcano-tectonic regions of S-Algeria, N-Mali and N-Niger, dike propagation from shallow magmatic chambers is controlled by the interaction with the local and regional stress fields, whereas their variations result from a combination of factors such as the geometry of pressurized magma chambers and the local geologic structure and the pre-existing fractures. When dike swarms are associated with flood basalts, their full extent and distribution are often difficult to assess because of a lack of exposure (Hou, 2011). Dike systems are typically hidden beneath volcanic piles or youngest sedimentary covers.

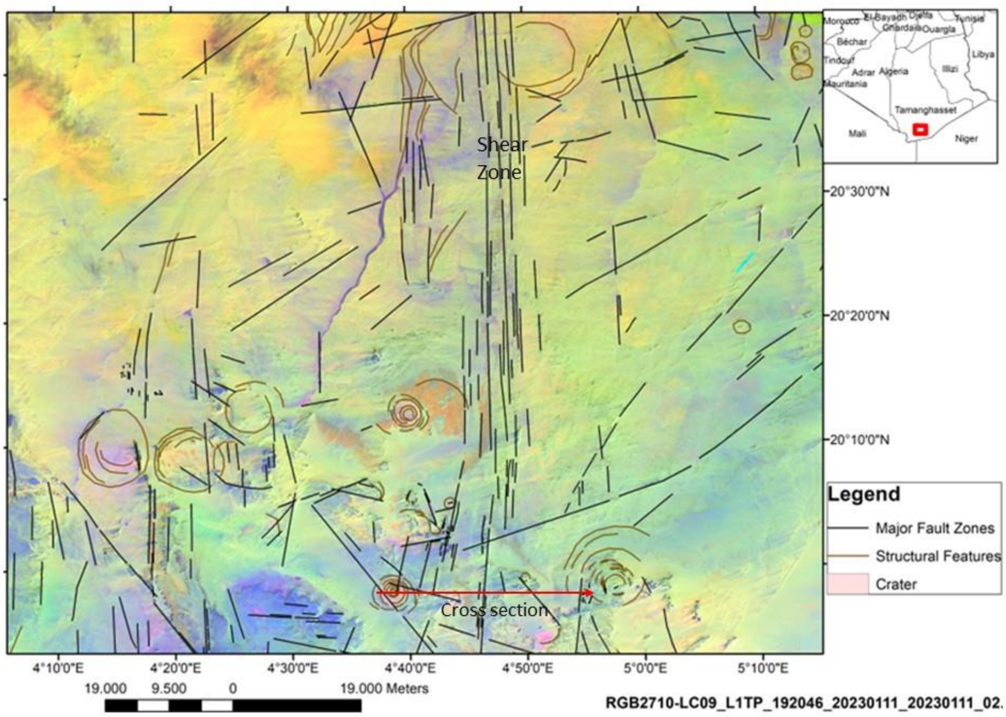

Figure 9. Structural Evaluation of the Scene in Figure 9

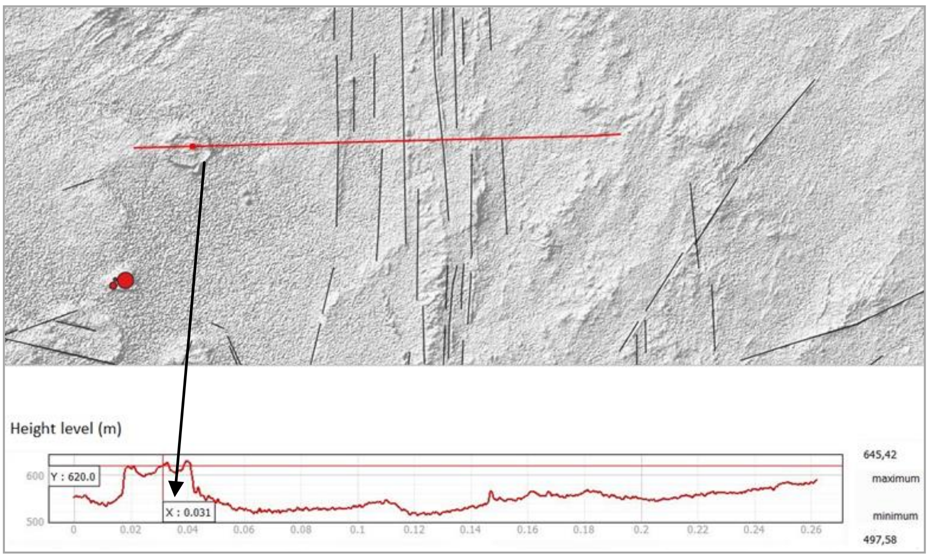

Figure 10. W-E-topographic Cross Section of The Shear Zone and the Crater (Left Side) Based on SRTM DEM Data

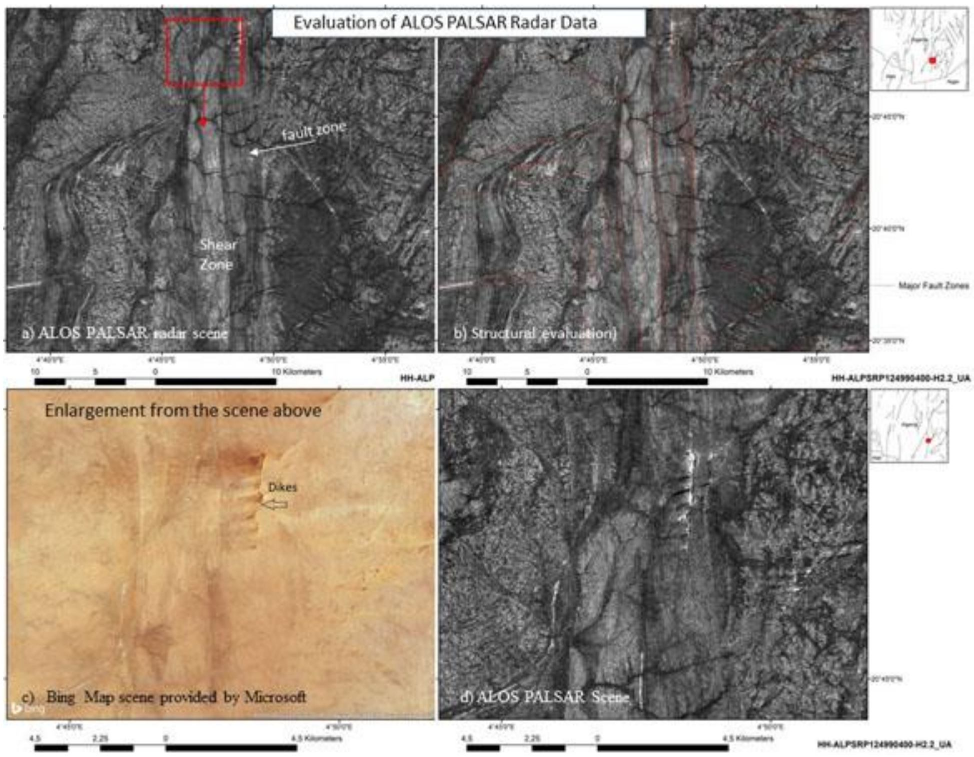

Figure 11. a) and b). ALOS PALSAR L-Band-scene (Horizontal Polarization HH) of a Large, Pan-African Shear Zone in the Hoggar Massif (Red Frame-enlargement Shown in c and d) c) BingMap, and d) ALOS PALSAR-Scenes visualizing Dikes along the Shear Zone in the SW of the Hoggar Mountains

An overview of dikes visible on the different satellite data is shown in the next figure (Figure 12 a and b). The density of dikes was calculated to visualize those areas with a higher dike concentration (Figure 12 a). The relatively higher dike density might be explained by uprising magma, that (by updoming the strata above) intensified fracturing processes and the reactivation of existing fault zones. Dikes intruded into these zones of weakness. The highest density of dikes striking predominantly NNW-SSE was detected in the Adrar des Iforas area in N-Mali (Figure 12 b) within the Kidal-terrane, mainly comprising basement gneisses and calc-alkaline granitic plutons (Bosch et al., 2016). A higher density of dikes could be used as an indicator for a relatively stronger tectonic stress in the affected area, at least at the time period of their development.

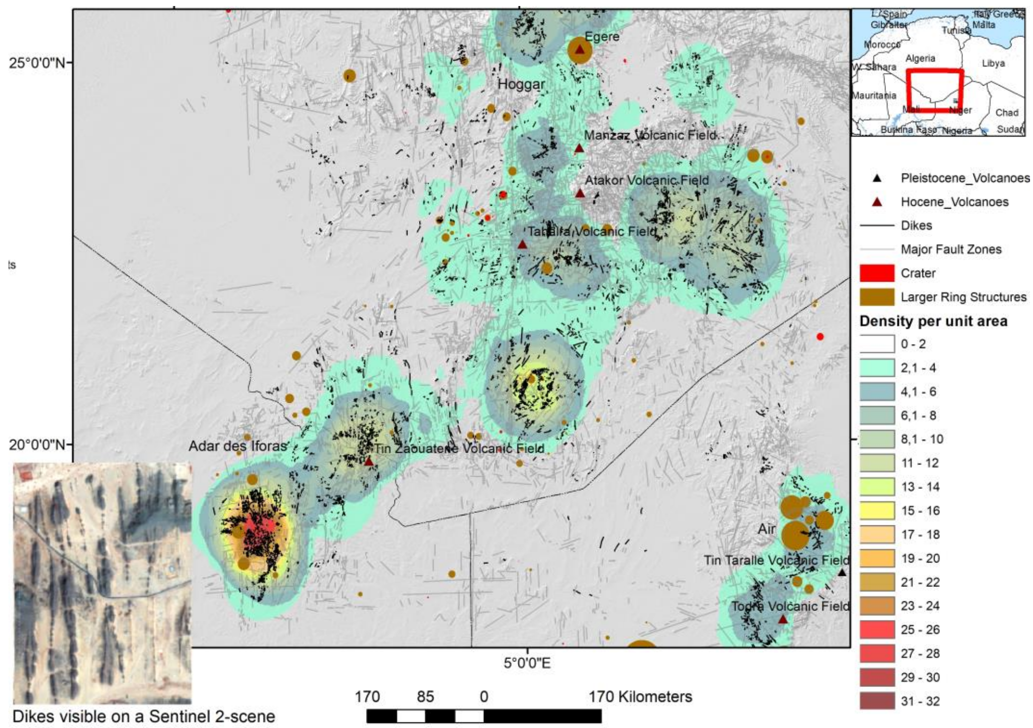

Figure 12 a. Density Concentration of Dikes Digitized Based on the Different Satellite Data

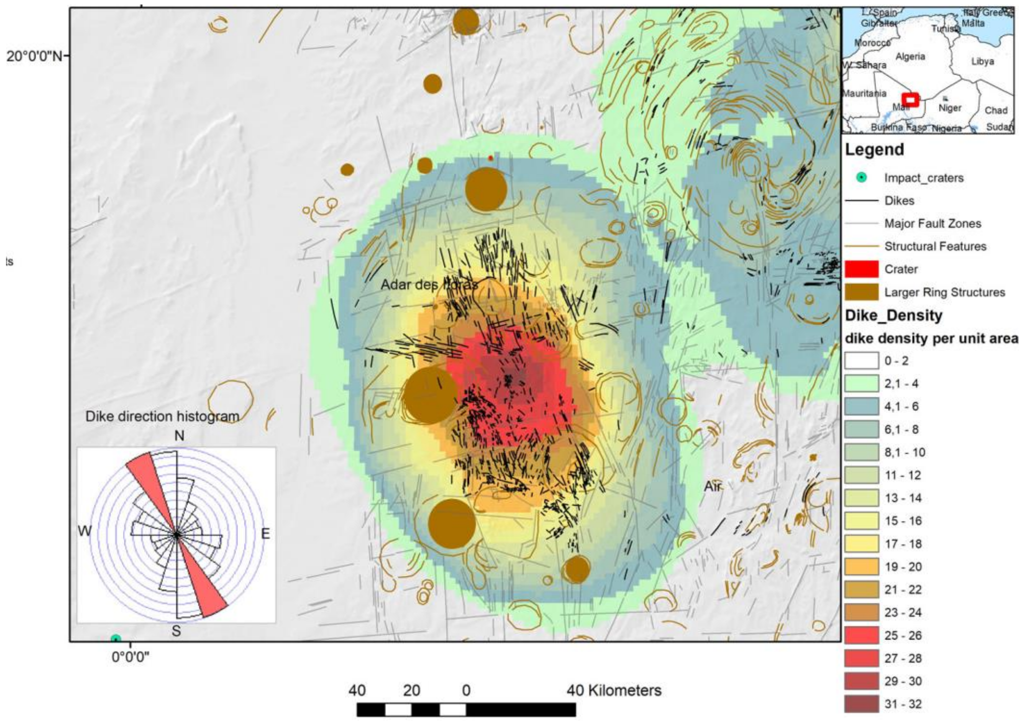

Figure 12 b. Highest Dike Density in the Adrar des Iforas Area in N-Mali and Main Dike Orientations

Larger circular structures appear on the different satellite images as demonstrated in the next figures.

3.1 Large Ring Structures Related To Plutons Visible By Traces of a Circular Outline Because of the Drainage Pattern and Circular Tonal Anomalies on the Satellite Images

Pluton emplacement mechanisms and surrounding conditions play an important role. The ring structures mostly related to alkaline magmatism (535-525 Ma) as described by Liégeois (2008) and the surrounding area are intruded later, mainly during the Cenozoic reactivation (35-0 Ma) by ring dikes, radial dikes and volcanic lava fields.

The advantage of radar images becomes evident as the drainage network and structural features are clearly traced on the Sentinel 1- C-Band radar image, whenever sheets of aeolian sediments are covering rock units as shown in Figure 13 a and b.

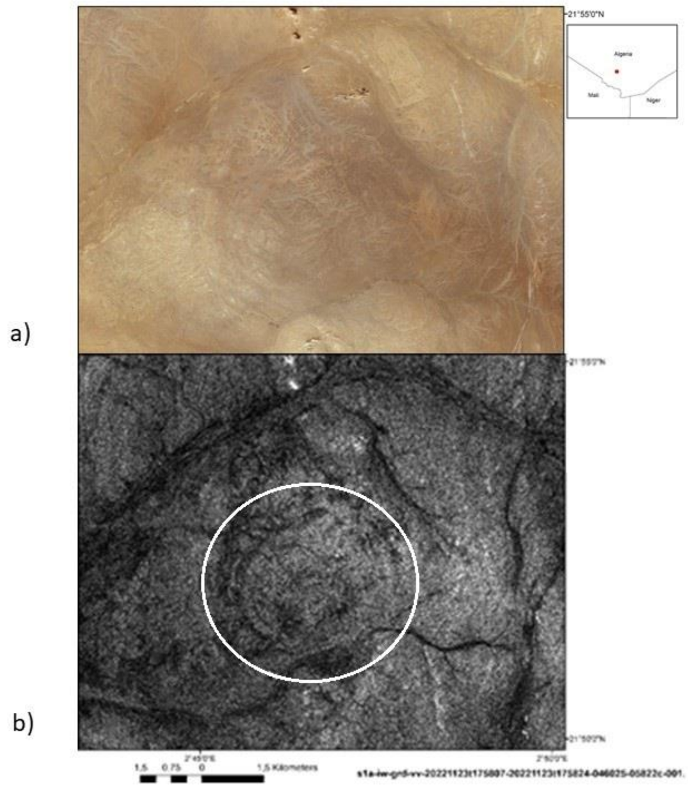

Figure 13 a and b. Comparison of a BingMap-scene with a Sentinel 1 Radar-scene Indicating a Buried Ring Structure in SW-Algeria

The Advanced Land Observing Satellite (ALOS) L-band Synthetic Aperture Radar (PALSAR, Japanese Space Agency-JAXA) complex single look (SLC) images are characterized by the optimal conditions of penetration in these desert areas depending on the grain size, rare moisture, surface roughness, radar backscattering mechanism and radar illumination geometry (Sieber & Theilen-Willige 1984; Theilen-Willige, 1986; Mansour et al., 2022). The ALOS/PALSAR L-band waves can propagate up to several meters, and, thus, may detect faults and structural features buried underneath loose sedimentary covers. The next figure (Figure 14) demonstrates the better evaluation feasibilities of the L-Band radar data to detect a circular structure in comparison with optical satellite data due to the traces of a concentric drainage pattern. Thus, circular structures nearly invisible in the field and on optical satellite images because of sedimentary covers can be detected and mapped precisely on the radar image. The detection of the drainage system underneath younger sedimentary covers plays a role in case of rare flash floods in these arid areas because the surface water infiltrates through the loose sediment covers predominantly into the older drainage systems and, thus, contributes to groundwater storage.

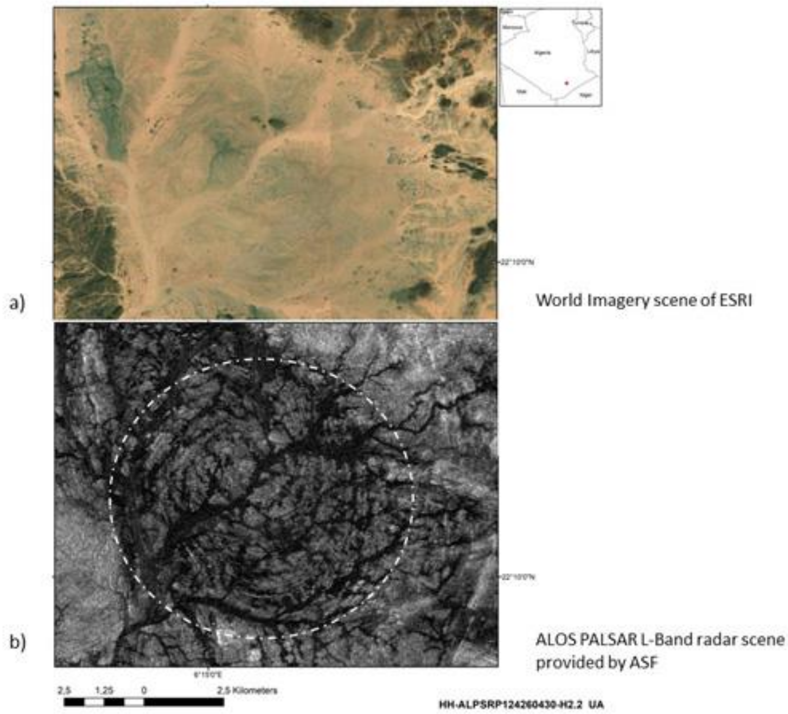

Figure 14 a and b. World Imagery-scene provided by ESRI (a) in Comparison with the ALOS PALSAR L-Band Single Horizontal Polarized (HH) Radar Scene (b) Indicating a Multi-ringed, Circular Structure Forming a Basin with a Diameter of about 8 km and a Concentric Drainage Pattern in SE-Algeria

Another example is presented in Figure 15 a, b, c and d by comparing optical satellite data with the ALOS PALSAR L-Band (single horizontal polarized-HH), radar scene showing traces of a multi-ringed structure in South-Algeria with a diameter of about 12 km. Whereas the optical satellite data such as Landsat (Figure 15 c) reveal "stripes" caused by wind erosion in the main wind direction, the radar image allows a more detailed insight of the structural setting. The origin of this structure can be explained by an uprising magmatic body updoming the strata above and leading to ring faults that are traced by the drainage pattern on the radar scene in dark concentric lines (Figure 15 b). However, this structure has a strong geomorphologic similarity with a complex cosmic impact crater as well by showing a central hill ring (central uplift?) surrounded by ring depressions and concentric hill ranges. There seems to be a ring graben outlining the structure. The ring structure was intersected later by dikes in the eastern part. This structure should be investigated in the field to get rock samples for mineralogic analysis to get more knowledge about its origin.

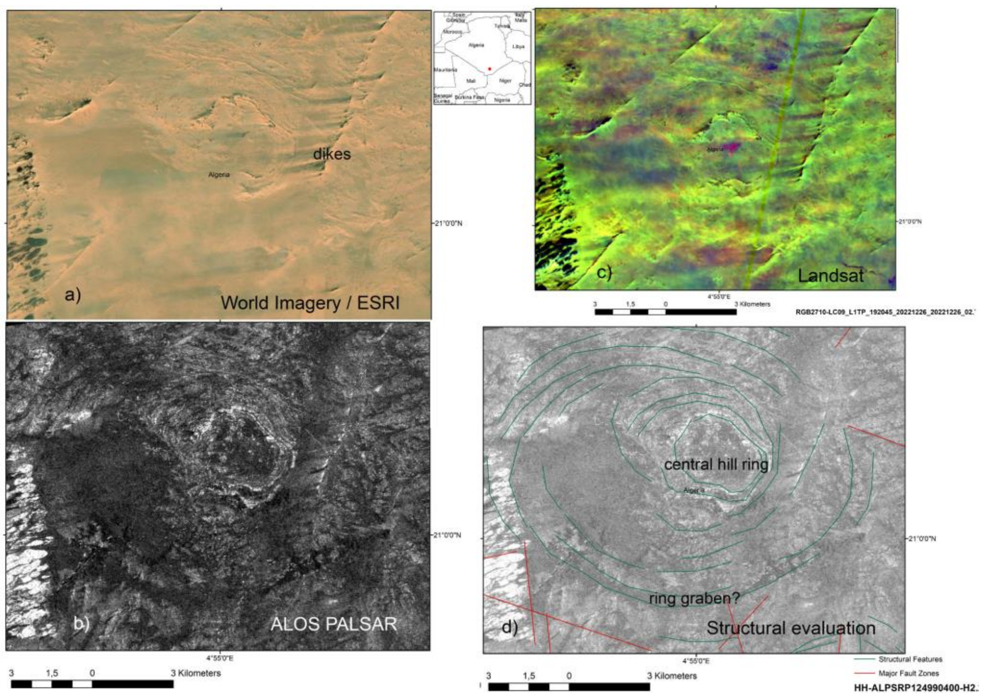

Figure 15 a-d. Detection of a Circular, Complex Structure in S-Algeria Based on Different Satellite Data

3.2 Larger Circular Basins and Depressions

The thermally emitted radiation or brightness temperature observed over deserts in Algeria supports the detection of reflection anomalies using satellite-based data. When evaluating Landsat 8 and 9 RGB images involving the thermal bands large circular basins with surrounding concentric hill ranges, often consisting of ring dikes, become clearly visible (Figure 16). Large basins with more than 10 km in diameter are intersected by younger, parallel dike intrusions and dike swarms.

3.3 Smaller Ring Structures in Volcanic Areas

Different volcanic fields are situated in the Hoggar mountains in South Algeria in height levels up to 3,000 meters with the lava domes and lava sheets, maars and scoria cones rising above the surrounding terrain. The topographic highlands are composed of Precambrian basement uplifted since the Pliocene and of overlying lava plateaus, domes and spines, scoria cones, and valley-filling lava flows. The scoria cones have similar morphologies, characterized by the formation of an external erosion cliff, 10 to 30 m high, carved in the ejecta. A pediment developed at the cliff base, about 100 m wide, surrounding the cones, often covered by aeolian sediments (Yahiaoui et al., 2014). Some are forming craters and maars.

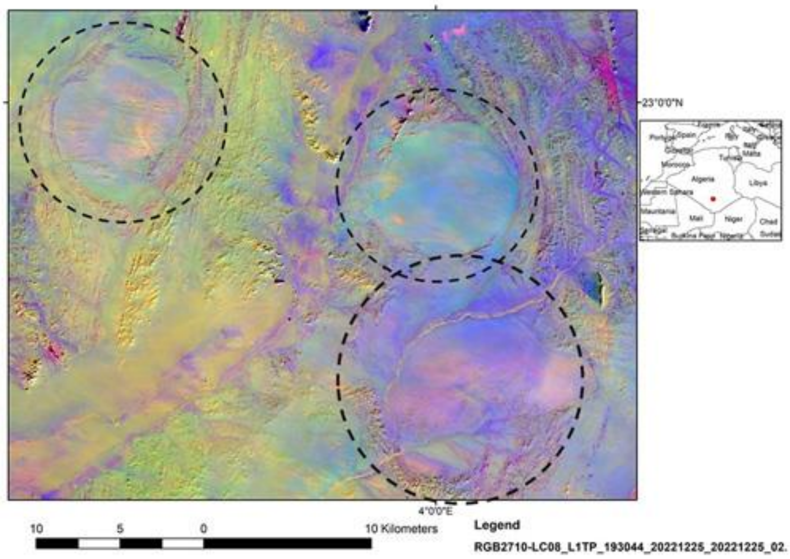

Figure 16. Landsat 8-RGB Scene of Ring-shaped Basins (Eroded Alkaline Domes) Surrounded by Ring Dikes in South Algeria

The Atakor massif is located at the center of the Hoggar swell within the Tuareg shield. It is characterized by volcanic activity during three discrete Neogene igneous episodes, separated by fairly long periods of quiescence (Azzouni-Sekkal et al., 2003, 2007). The evaluation of optical and radar satellite data contributes to a more detailed knowledge of the deep-seated fault zones facilitating the uprise of magmatic intrusions. In the area of the Atakor and Tahalra volcanic field prominent W-E and N-S oriented lineaments are prevailing (Figure 17, Figure 18). The lavas lie on Precambrian granitic and gneissic rocks (Azzouni-Sekkal et al., 2007). Uprise of magma occurred predominantly where N-S striking, large shear zones are intersected by W-E oriented lineaments. Whereas the occurrence of volcanic activities in the Atakor and Tahalra fields seem to be influenced by larger fault zones, the next examples of the Egéré volcanic field, Idlès, Tamanrasset Province, show the influence of pre-existing ring structures such as domes with concentric faults on the emplacement of younger magmatic bodies as well (Figure 19 a and b). Developmental sequences of intrusions can be observed. The concentric arrangement of scoria cones follows both, the ring faults and larger intersecting fault zones.

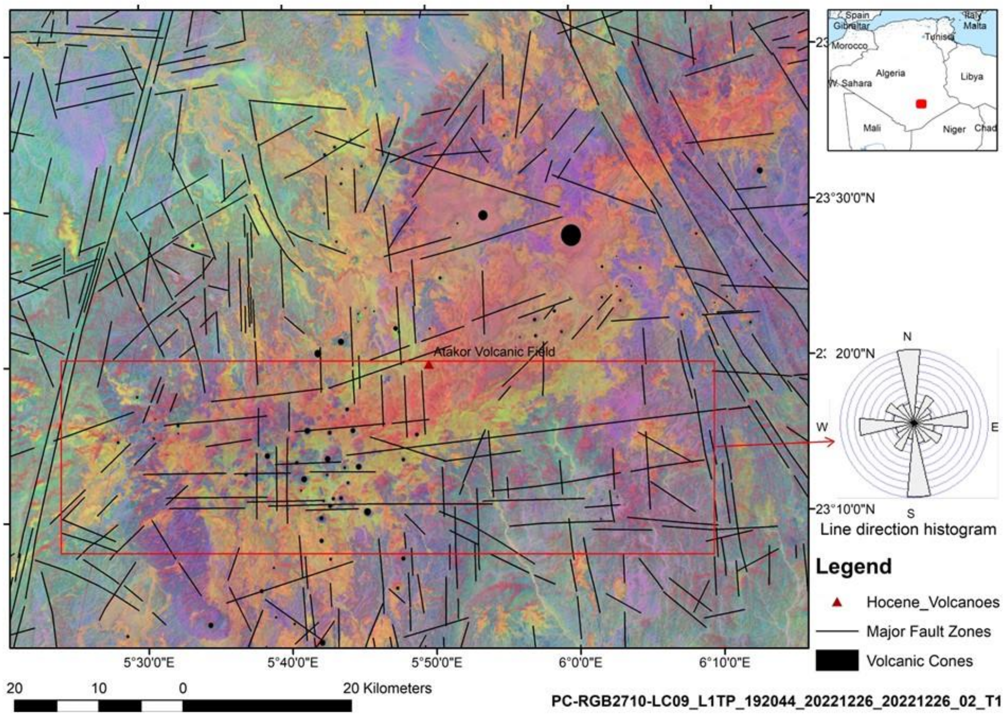

Figure 17. Structural Analysis Based on Optical and Radar Satellite Images of The Atakor Volcanic Field (Landsat 9-RGB Image in the Background Indicating Lava Fields in Orange and Yellow Colors). The Line Direction (Rose) Diagram Is Calculated Based on Lineaments in the Red Indicated Area

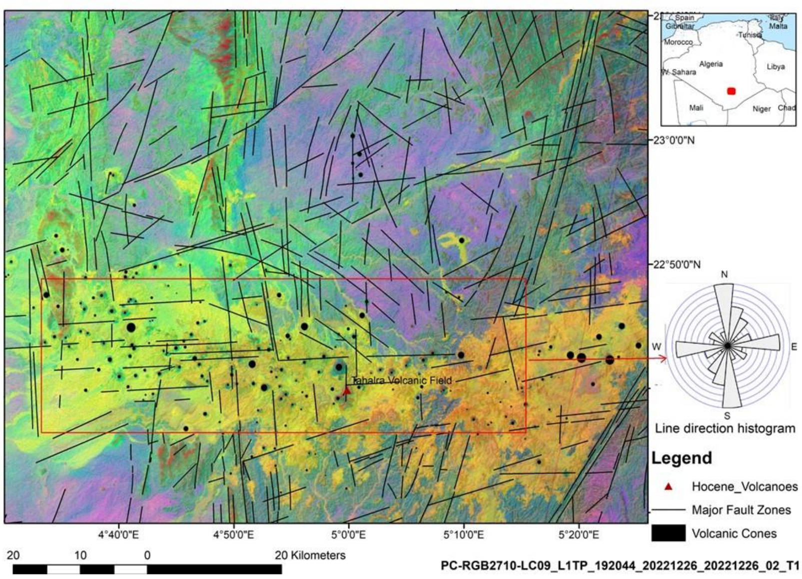

Figure 18. Structural Analysis of the Talhara Volcanic Field Based On Satellite Data

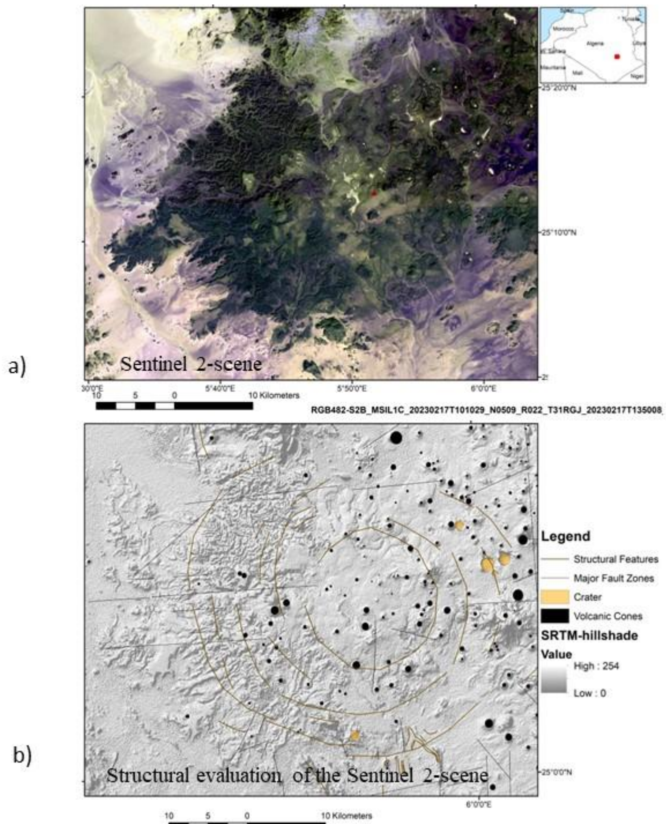

Figure 19 a and b. Sentinel 2-scene of the Western Part of the Egéré Volcanic Field (a) with a Concentric Arrangement of the Scoria Cones and Lava Fields and (b) Structural Evaluation of the Sentinel 2-scene

3.4 Smaller Cosmic Impact Craters

Most of the documented known impact craters in the investigation area are smaller, bowl-shaped, simple impact craters such as the Talemzane crater in N-Algeria (Figure 20). The Talemzane crater is embedded in in Senonian or Eocene limestones and features an up to 70 m high rim. Limestones are strongly fractured, upturned, and -in the upper rim-overturned. Large, ejected blocks of limestone are scattered around the outside of the crater. Breccia dikes are intersected by the crater wall, and detrital or reworked monomict breccia is found at the crater floor near the rim. Quartz is a rare constituent in the limestones, but Lambert et al. (1980) reported high pressure modifications like planar elements in some quartz grains. These authors estimated the age of the structure at <3 Ma because of the limited degree of erosion observed (Reimold & Köberl, 2014).

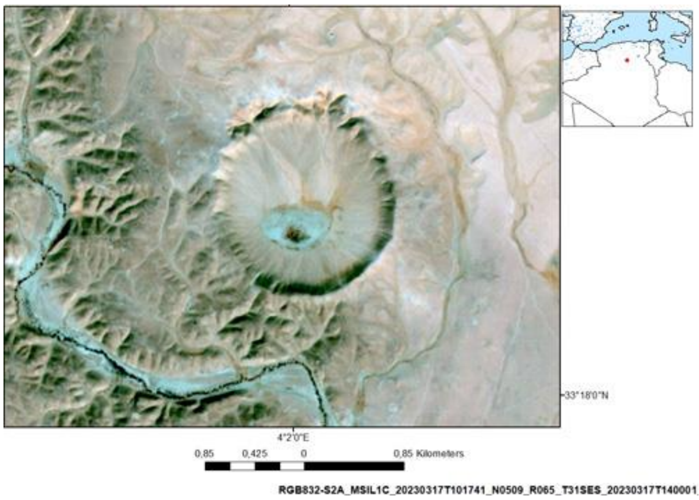

Figure 20. Sentinel 2-RGB-scene of the Talemzane Impact Crater

The next figure (Figure 21 a) provides an overview of ring structures forming craters, most of them related to magmatic activity (maars, calderas). However, some of them might be related to cosmic impacts. Figure 21 b shows the diameter of crater-shaped ring structures, most of them with a diameter of about < 1 km, up to 1-2 km. When evaluating the different satellite data further craters were identified that are assumed to be created by a cosmic impact due to their similarities to the known impact craters and should be recommended for more detailed mineralogical and geophysical investigations to verify their origin. Examples of craters that might be formed by a cosmic impact and not documented so far are presented in the next figures (Figure 22 and Figure 23), a potential complex crater with a diameter of about 4 km in Figure 24.

As mineral deposits are often linked to these types of ring structures (Reimold & Koeberl, 2005; Osinski et al., 2012), more detailed investigations would make sense. The evaluation of different satellite data helps to focus cost- and time-intensive field research.

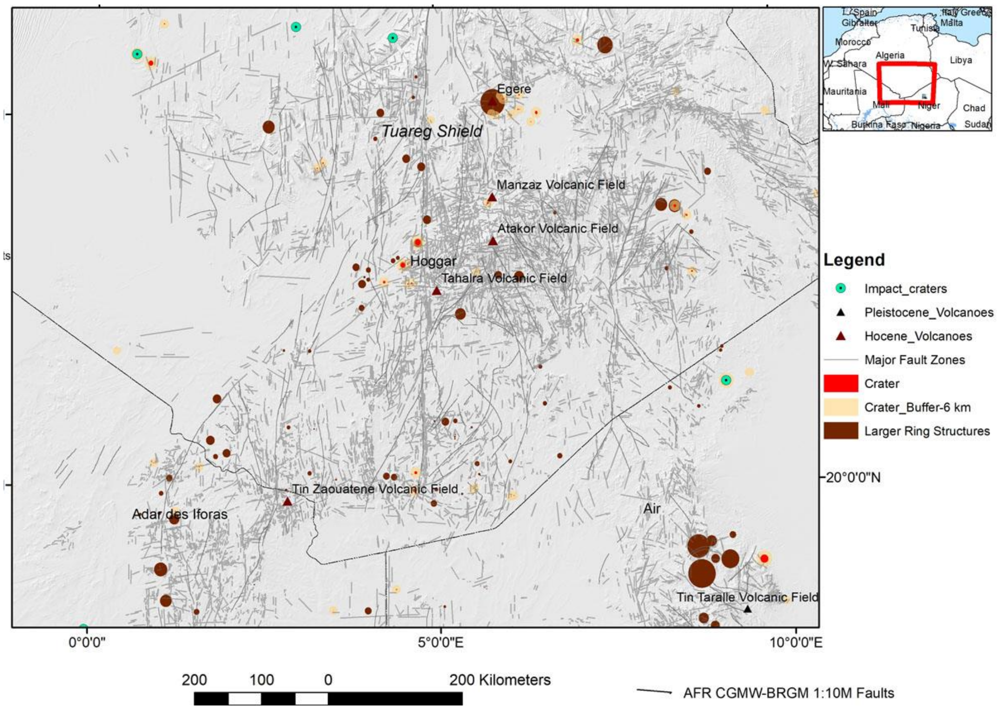

Figure 21 a. Ring Structures with Crater Morphology (Red Points)

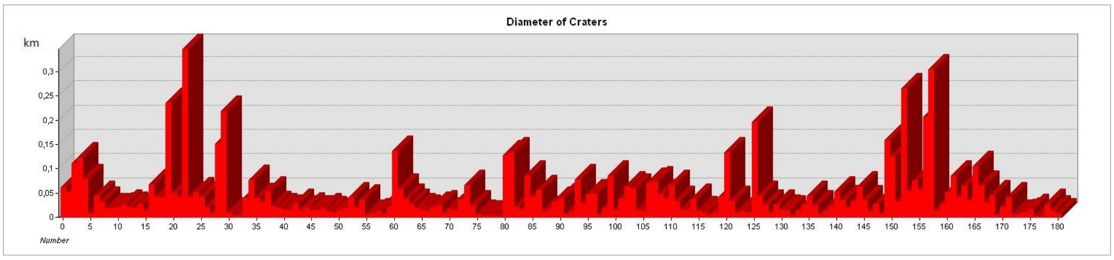

Figure 21 b. Diameters of Crater-like Ring Structures

5. Conclusions

Evaluations of different satellite data, enhanced with digital image processing methods, allow a more detailed and systematic inventory of circular structures, their different types, sizes and their surrounding tectonic pattern, even the detection of so far unknown ring structures. When analyzing the different satellite data, it becomes obvious that majority of the larger ring structures can be identified and correlated with available geologic information, whereas the smaller circular features (with exception of those situated within volcanic areas) are sometimes difficult to determine regarding their origin. Nevertheless, the inventory of circular features based on satellite images will support further investigation in the field by providing a data base for focused field research. In the arid environment of the investigation area ALOS PALSAR L-Band data were especially useful for this purpose because of the penetration capability of long-wave radar signals into dry, loose sedimentary covers.

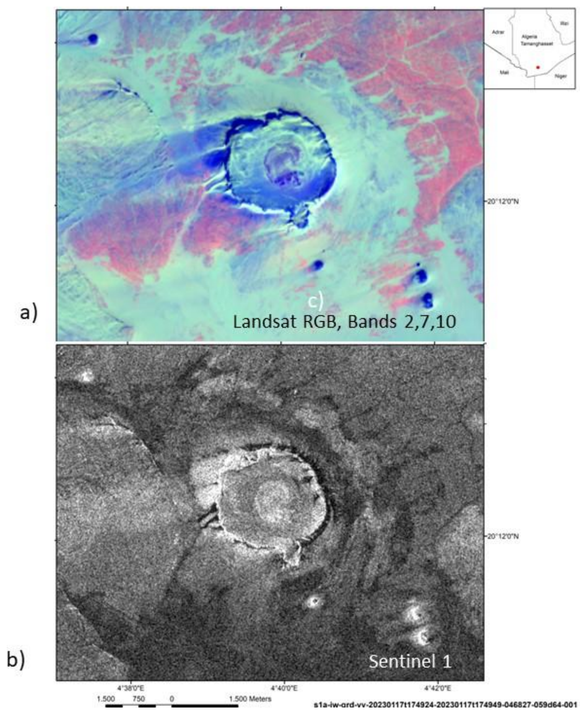

Figure 22 a and b. Landsat 9- and Sentinel 1-scene of a Potential Impact Crater in S-Algeria

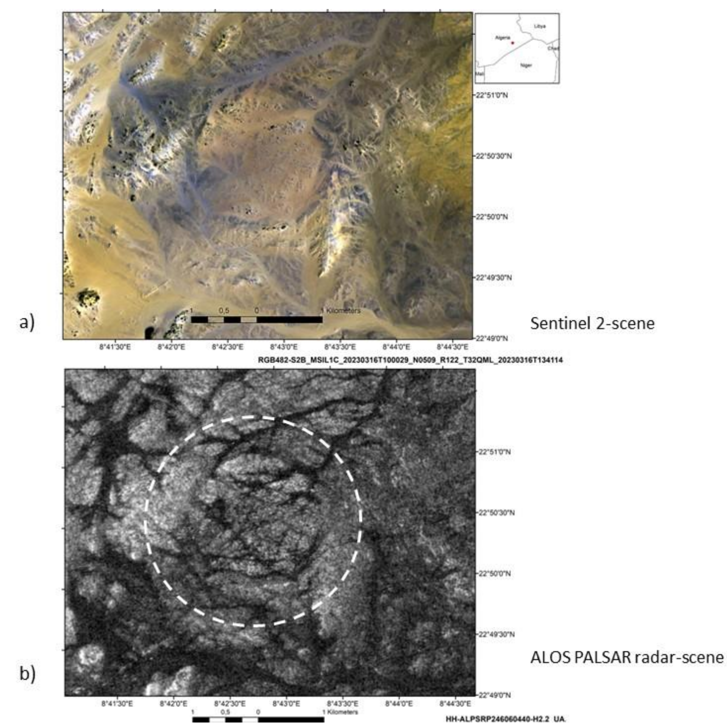

Figure 23. Sentinel 2-scene of a Potential Eroded Impact Crater Site in SE-Algeria, a Ring Structure with a Diameter of about 2 km, Embedded in Paleoproterozoic Calc-alkaline Plutonic and Anatectic Layers and Neoproterozoic to Ordovician Sedimentary Layers (according to CGMW-BRGM 1:10M Geological Map of Africa,-3rd Edition)

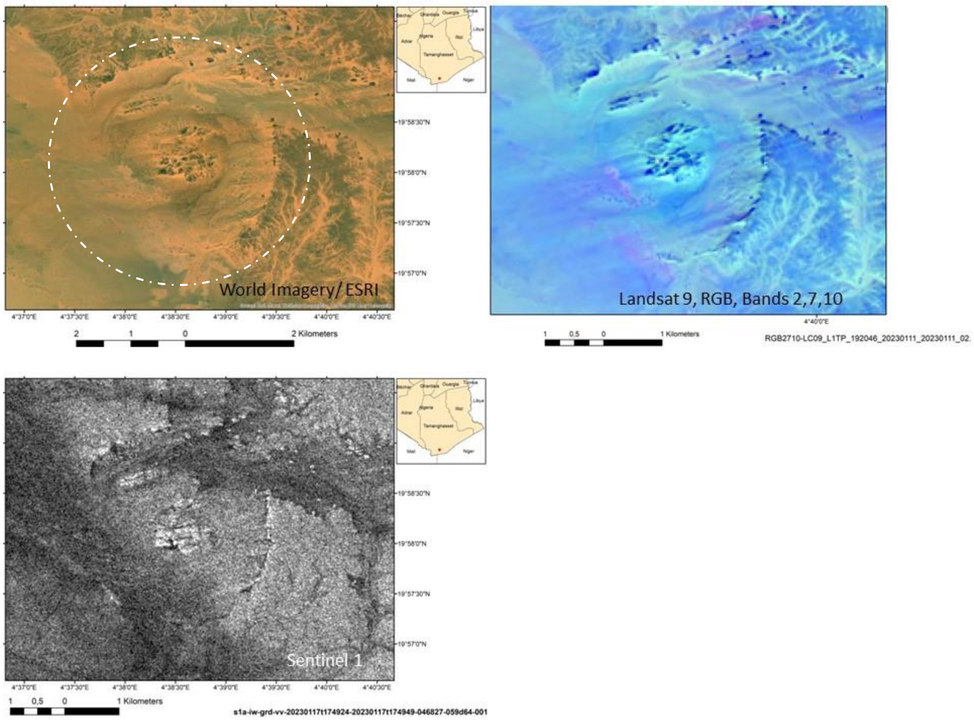

Figure 24. Satellite-scenes of a Potential Complex Impact Crater in S-Algeria with a Central Elevation (?)

Acknowledgement

The author is grateful for the input and support of the editor and team of *Energy and Earth Science* and the reviewers.

References

Alaska Satellite Facility (ASF). (n.d.). *Data Search Vertex*. NASA Earth Data. Retrieved from https://search.asf.alaska.edu/#/

Amara, M., Hamoudi, M., Djemaï, S., Bendaoud, A., Dufréchou, G., Jessell, W. M., Boubekri, H., Ouzegane, K., Guemmama, M., & Machane, D. (2017). New insight of the geological structures and tectonic framework of Ahnet and northwestern part of Tin Zaouatine terranes (western Hoggar, Algeria) constraints from aeromagnetic, gamma ray, and remote sensing data. *Arab J Geosci.*, *10*, 396. https://doi.org/10.1007/s12517-017-3060-7

Attwa, M., El Bastawesy, M., Ragab, D., Othman, A., Assaggaf, H. M., & Abotalib, A. Z. (2021). Toward an Integrated and Sustainable Water Resources Management in Structurally-Controlled Watersheds in Desert Environments Using Geophysical and Remote Sensing Methods. *Sustainability*, *13*, 4004. https://doi.org/10.3390/su13074004

Azzouni-Sekkal, A., Bonin, B., Benhallou, A., Yahiaoui, R., & Liégeois, J. P. (2007). Cenozoïc alkaline volcanism of the Atakor Massif (Hoggar, Algeria). *Geological Society of America, Special Paper of the Geological Society of America*, *418*, 321-340. https://doi.org/10.1130/2007.2418(16)

Azzouni-Sekkal, A., Liégeois, J. P., Bechiri-Benmerzoug, F., Belaidi-Zinet, S., & Bonin, B. (2003). The "Taourirt" magmatic province, a marker of the closing stage of the Pan-African orogeny in the Tuareg Shield: Review of available data and Sr-Nd isotope evidence. *Journal of African Earth Sciences*, *37*, 331-350. https://doi.org/10.1016/j.jafrearsci.2003.07.001

Black, R., & Liégeois, J. P. (1993). Cratons, Mobile Belts, Alkaline Rocks and Continental Lithospheric Mantle: The Pan-African Testimony. *Journal of the Geological Society*, *150*, 89-98. https://doi.org/10.1144/gsjgs.150.1.0088

Black, R., Bamako, H. B., Ball, E., Bertrand, J. M., Boullier, A. M., Caby, R., Davidson, I., Fabre, J., Leblanc, M., & Wright, L. I. (1979). Outline of the Pan-Aftrican Geology of Adrar des Iforas (Republic of Mali). *Geol.Rundschau*, *68*(2), 543-564. https://doi.org/10.1007/BF01820806

Black, R., Latouche, L., Liégeois, J. P., Caby, R., & Bertrand, J. M. (1994). Pan-African displaced terranes in the Tuareg Shield (central Sahara). *Geology*, *22*(7), 641-644. https://doi.org/10.1130/0091-7613(1994)022<0641:PADTIT>2.3.CO;2

Bosch, D., Bruguier, O., Caby, R., Buscail, F., & Hammor, D. (2016). Orogenic development of the Adrar des Iforas (Tuareg Shield, NE Mali): New geochemical and geochronological data and geodynamic implications. *Journal of Geodynamics*, *96*, 104-130. https://doi.org/10.1016/j.jog.2015.09.002

Bougrine, A., Yelles-Chaouche, A. K., & Eric, C. (2019). Active deformation in Algeria from continuous GPS measurements. *Geophys. J. Int.*, *217*, 572-588. https://doi.org/10.1093/gji/ggz035

Bouzid, A., Bayou, B., Liégeois, J.-P., Bourouis, S., Bougchiche, S. S., Bendekken, A., Abtout, A., Boukhlouf, W., & Ouabadi, A. (2015). Lithospheric structure of the Atakor metacratonic volcanic swell (Hoggar, Tuareg Shield, southern Algeria): Electrical constraints from magnetotelluric data. In G. R. Foulger, M. Lustrino, & S. D. King (Eds.), *The Interdisciplinary Earth: A Volume in Honor of Don L. Anderson: Geological Society of America Special Paper 514 and American Geophysical Union Special Publication 71* (1-XXX).

Chabou, M. C. (2009). Le cratère météoritique de Talemzane (Daïet el Maadna). *La Lettre du CRAAG, Centre de Recherche en Astronomie, Astrophysique et Géophysique Trimestrielle d'information*, *juillet*, *2009*(45), 4-5.

English, K. L., Redfern, J., Bertotti, G., Joseph, M., English, J. M., & Cherif, R. Y. (2016). Intraplate uplift: New constraints on the Hoggar dome from the Illizi basin (Algeria). *Basin Research*, 1-17. https://doi.org/10.1111/bre.12182

European Space Agency (ESA). (n.d.). *Copernicus Open Access Hub*. Retrieved from https://scihub.copernicus.eu/dhus/#/home

Fezaa, N., Liégeois, J. P., Abdallah, N., Cherfouh, E. H., De Waele, B., Bruguier, O., & Ouabadi, A. (July 2010). Late Ediacaran geological evolution (575-555 Ma) of the Djanet Terrane, Eastern Hoggar, Algeria, evidence for a Murzukian intracontinental episode. *Precambrian Research*, *180*(3-4), 299-327. https://doi.org/10.1016/j.precamres.2010.05.011

Geofabrik's free download server. (n.d.). Retrieved from http://download.geofabrik.de/africa.html

Hou, G. (2011). Mechanism for three types of mafic dyke swarms. *Geoscience Frontiers*, *3*(2), 217-223. https://doi.org/10.1016/j.gsf.2011.10.003

Kourim, F., Bodinier, J. L., Alard, O., Bendaoud, A., Vauchez, A., & Dautria, J. M. (2014). Nature and Evolution of the Lithospheric Mantle beneath the Hoggar Swell (Algeria): A Record from Mantle Xenoliths. *Journal of Petrology*, *55*, 2249-2280. https://doi.org/10.1093/petrology/egu056

Lambert, P., McHone, J. F., Dietz, R. S., & Houfani, M. (1980). Impact and impact-like structures in Algeria, Part I, Four bowl-shaped depressions. *Meteoritics*, *15*, 157-179. https://doi.org/10.1111/j.1945-5100.1980.tb00518.x

Lambert, P., McHone, J. F., Dietz, R. S., Briedj, M., & Djender, M. (1981). Impact and impact-like Structures in Algeria, Part II, Multi-ringed Structures. *Meteoritics*, *16*(3), 203-227. https://doi.org/10.1111/j.1945-5100.1981.tb00546.x

Liégeois, J. P. (2008). *The Hoggar swell and volcanism, Tuareg shield, Central Sahara: Intraplate reactivation of Precambrian structures as a result of Alpine convergence*. Retrieved from http://www.mantleplumes.org/Hoggar.html

Liégeois, J. P., Benhallou, A., Azzouni-Sekkal, A., Yahiaoui, R., & Bonin, B. (2005). The Hoggar swell and volcanism: Reactivation of the Precambrian Tuareg shield during Alpine convergence and West African Cenozoic volcanism. In G. R. Foulger, J. H. Natland, D. C. Presnall, & D. L. Anderson (Eds.), *Plates, plumes, and paradigms. Geological Society of America Special Paper*, *388*, 379-400.

Liegeois, J. P., Latouche, L., Boughrara, M., Navez, J., & Guiraud, M. (2003). The LATEA metacraton (Central Hoggar, Tuareg shield, Algeria): Behaviour of an old passive margin during the Pan-African orogeny. *Journal of African Earth Sciences*, *37*, 161-190. https://doi.org/10.1016/j.jafrearsci.2003.05.004

Mansour, K., Abdel, Z. M., Al deep, M., Medhat, N., Ebrahim, S., & Mohamed, A. (2022). Validation of ALOS/PALSAR subsurface penetration depth in arid regions based on field ground penetrating radar measurements. *Research Square*, July 28th, 2022, 1-15. https://doi.org/10.21203/rs.3.rs-1877140/v1

Moreau, C., Demaiffe, D., Bellion, Y., & Boullier, A. M. (1994). A tectonic model for the location of Palaeozoic ring complexes in Aïr (Niger, West Africa). *Tectonophysics*, *234*(1-2), 129-146.

https://doi.org/10.1016/0040-1951(94)90208-9

OneGeology portal, British Geological Survey. (n.d.). Retrieved from http://portal.onegeology.org/OnegeologyGlobal/

Osinski, G. R., Tornabene, L. L., Banerjee, N. R., Cockell, C. S., Flemming, R., Izawa, M. R. M., McCutcheon, J., Parnell, J., Preston, L. J., Pickersgill, A. E., Pontefract, A., Sapers, H. M., & Gordon, S. (2012). Impact-generated hydrothermal systems on Earth and Mars. *Icarus*, *224*(2), 347-363. https://doi.org/10.1016/j.icarus.2012.08.030

Paillou, P. (2017). Mapping Palaeohydrography in Deserts: Contribution from Space-Borne Imaging Radar. *Water 2017*, *9*, 194. https://doi.org/10.3390/w9030194

Paillou, P., Reynard, B., Malezieux, J. M., Dejax, D., Heggy, E., Rochette, P., Reimold, W. U., Michel, P., Baratoux, D., Razin, P., & Colin, J. P. (2006). An extended field of crater-shaped structures in the Gilf Kebir region, Egypt: Observations and hypotheses about their origin. *Journal of African Earth Sciences*, *46*, 281-299. https://doi.org/10.1016/j.jafrearsci.2006.05.006

Planetary and Space Science Centre (PASSC), Canada. (n.d.). *Earth Impact Database—Africa*. Retrieved from http://www.passc.net/EarthImpactDatabase/New%20website_052018/Africa.html

Reimold, W. U., & Koeberl, C. (2014). Impact structures in Africa: A review. *Journal of African Earth Sciences*, *93*(2014), 57-175. https://doi.org/10.1016/j.jafrearsci.2014.01.008

Reimold, W. U., Koeberl, C., Gibson, R. L., Burkhard, O., & Dressler, B. O. (2005). Economic Mineral Deposits in Impact Structures: A Review. In C. Koeberl, & H. Henkel (Eds.), Impact Tectonics. Impact Studies, *6*, 479-552. https://doi.org/10.1007/3-540-27548-7_20

Sieber, A., & Theilen-Willige, B. (1984). Comparative geologic Analysis of Landsat and SIR-A-Images of the Adrar des Iforas Area in Mali. In *Conference: Proceedings of IGARSS' 84 Symposium* (27-30 August 1984, Ref. ESA SP-215 (published by ESA Scientific & Technical Publications Branch in August 1984, Strasbourg), pp. 237-240).

Theilen-Willige, B. (1986). Satelliten-Radaraufnahmen als Hilfsmittel bei der Erfassung von Entwässerungssystemen in Nordafrika und Vorderasien. *Zeitschrift der Deutschen Geologischen Gesellschaft (Z.dt.geol.Ges)*, *137*(1), 363-377. https://doi.org/10.1127/zdgg/137/1986/363

Theilen-Willige, B. (2023). Inventory of Ring Structures in N- and W-Morocco based on Satellite Data. *European Journal of Environment and Earth Sciences*, *4*(1), 34-45. https://doi.org/10.24018/ejgeo.2023.4.1.364

USGS Earth Explorer. (n.d.). Retrieved from https://earthexplorer.usgs.gov/

Yahiaoui, R., Dautria, J. M., Alard, O., Bosch, D., Azzouni-Sekkal, A., & Bodinier, J. L. (2014). A volcanic district between the Hoggar uplift and the Tenere Rifts: Volcanology, geochemistry and age of the In-Ezzane lavas (Algerian Sahara). *Journal of African Earth Sciences*, *92*, 14-20. https://doi.org/10.1016/j.jafrearsci.2013.12.001